Recent Results of an Investigation of Mach Effect Thrusters

Heidi Fearn[1] and James F. Woodward[2]
California State University, Fullerton, CA, 92834

The theory underlying Mach effects – fluctuations of the restmasses of accelerating objects in which internal energy changes take place – and their use for propulsion is briefly recapitulated. Experimental apparatus based on a very sensitive thrust balance is briefly described. The experimental protocol employed to search for expected Mach effects is laid out, and the results of this experimental investigation are presented. A series of tests conducted to explore the origin of the thrust signals seen are described, and two of those tests – the most likely spurious sources of thrust signals – are considered in some detail. The thrust signals seen, if genuine Mach effects, suggest that "advanced and exotic" propulsion can be achieved with realistic resources.

Nomenclature

$\mathbf{A}_g$	=	gravimagnetic (three) vector potential
a	=	acceleration (bold: three vector acceleration)
c	=	vacuum speed of light
∇	=	gradient operator
δm_0	=	mass fluctuation
$d\mathbf{s}$	=	distance differential
E	=	energy
$\mathbf{E}_g$	=	gravelectric field strength
$\mathbf{F}$	=	three vector accelerating force
F	=	four vector gravitational field strength
f	=	three vector (spatial) gravitational field strength
G	=	Newton's constant of universal gravitation
K_p	=	piezoelectric constant (d_{33})
K_e	=	electrostriction constant
m	=	mass
M	=	mass of the universe
P	=	power
ϕ	=	scalar gravitational potential
r	=	radial distance
R	=	radius of the universe
ρ	=	"matter" density
$\mathbf{v}$	=	three velocity
V	=	volume, or voltage (context dependent)

I. Introduction

In 1953, Dennis Sciama published a paper, "On the Origin of Inertia" in the *Monthly Notices of the Royal Astronomical Society* wherein he resuscitated Einstein's idea that the inertia of material objects should be accounted for by a field interaction with the chiefly distant matter in the cosmos.[1] He did not use Einstein's theory of gravity, general relativity theory, to convey the interaction. Rather, he proposed a vector theory of gravity modeled on Maxwell's formalism for electrodynamics. Eventually, it was recognized that Sciama's vector formalism was just an approximation to Einstein's general relativity theory. But the simplicity and transparency of

---

[1] Professor, Department of Physics.
[2] Emeritus Professor of History and Adjunct Professor of Physics, Department of Physics, Senior Member AIAA.

the vector formalism made plain what was involved in explaining inertial effects as gravitational interactions with chiefly distant "matter" in the universe.

At the most elementary level, if we seek to show that inertial effects are the consequence of the gravitational action of chiefly distant matter in the cosmos, we must show that when a "test particle" is accelerated by an "external" force, the action of gravity due to all of the "matter" in the cosmos just produces the reaction force that opposes the external accelerating force required by Newton's third law of mechanics. If that is true, and the theory is locally Lorentz invariant, then we can be confident that all of the inertial effects of classical mechanics will follow. We first define the quantities set off in quotation marks in the preceding sentence. A test particle is a massive object, acted upon by the gravity of other objects, of sufficiently small mass that its gravitational effect on other objects is negligible. An external force on the test particle is produced by some agent that is not a part of the test particle. And matter here is understood as everything that gravitates. This, by Einstein's second law: $m = E/c^2$, includes all forms of *non-gravitational* energy, including zero restmass radiation. Gravitational energy, for some observers, contributes to m, but only in special circumstances as changes in the locally measured gravitational potential are unobservable in general relativity theory.

Sciama, for a set of idealized circumstances, showed that gravity does indeed account for inertial reaction forces provided certain conditions are fulfilled. He considered a test particle in a universe of uniform matter density and asked, what is the "gravelectric" force exerted on the test particle by the uniformly distributed matter? In analogy with Maxwell's electrodynamics, the gravelectric field strength $\mathbf{E}_g$ is given by:

$$\mathbf{E}_g = -\nabla\phi - \frac{1}{c}\frac{\partial \mathbf{A}_g}{\partial t}.$$

(1)

If the only term on the RHS of Equation (1) were that involving the scalar gravitational potential, we would be dealing with Newton's gravity theory. But since our theory of gravity is a vector theory, we have the additional term involving the gravitational vector potential, $\mathbf{A}_g$, an inductive term that arises from the "gravi" or "gravito" magnetic part of the interaction. Again, in analogy with electrodynamics, $\mathbf{A}_g$ has matter *currents* as its source, that is:

$$\mathbf{A}_g = \frac{G}{c}\int_V \frac{\rho \mathbf{v}}{r}dV.$$

(2)

where the matter current in a small volume element dV of space is the product of ρ, the matter density, and $\mathbf{v}$ its velocity at that location. The integration is to be carried out over all space. In electrodynamics, this integral vanishes because the electric charge density is, on average, zero. As Sciama remarked, this is not the case for gravity as there is no negative matter with non-vanishing cosmic scale density. So $\mathbf{A}_g$ will not vanish if $\mathbf{v}$ is not zero. Note that the distance dependence of $\mathbf{A}_g$ is $1/r$. This is the signature of a radiative interaction. It is, however, many orders of magnitude larger than customary gravitational radiative effects: quadrupole gravity waves.

Sciama noted that if we choose the instantaneous frame of rest of the test particle, the rest of the universe can be regarded as rigidly moving past the test particle with velocity $-\mathbf{v}$, so $\mathbf{v}$ can be removed from the integral in Equation (2). The remaining integral is just that which produces the total gravitational scalar potential at the location of the test particle, and,

$$\mathbf{A}_g = \frac{G}{c}\int_V \frac{\rho \mathbf{v}}{r}dV = \frac{1}{c}\frac{GM}{R}\mathbf{v} = \frac{\varphi}{c}\mathbf{v}.$$

(3)

Substitution for $\mathbf{A}_g$ in Equation (1) produces,

$$\mathbf{E}_g = -\nabla\phi - \frac{1}{c}\frac{\partial \mathbf{A}_g}{\partial t} = -\nabla\phi - \frac{\phi}{c^2}\frac{\partial \mathbf{v}}{\partial t}.$$

(4)

In the idealized circumstances considered by Sciama, the gradient of the scalar potential vanishes, as does the curl of the gravimagnetic field. So too does the second term in Equation (4) if the velocity is either zero or constant. If the test particle (or universe, depending on reference frame chosen) is accelerating, however, $\partial \mathbf{v} / \partial t$ does *not* vanish. And if ϕ / c^2 is equal to one, then the gravelectric field exactly produces the inertial reaction force conveyed through the test particle and felt by the accelerating agent.

Now, two things must be true if gravity is to account for inertial forces. First (and foremost), the condition $\phi / c^2 = 1$ must always and everywhere be true. And second, the simple vector approximation of Sciama must be replicated when the more elaborate formalism of general relativity theory is employed. We take the first criterion first. We know, from both special and general relativity theory, that c is a "locally measured invariant". That is, whenever a measurement of c is made with "local" apparatus, the number 3 X 10^8 m/s is recovered. If $\phi / c^2 = 1$ and c is a locally measured invariant, then it must be true that ϕ is a locally measured invariant equal to c^2. Is this correct? Yes, it was shown to be true by Carl Brans in 1962 when he corrected an earlier argument by Einstein that gravitational potential energy should alter the locally measured masses of objects.[2] This is the "non-localizability" of gravitational potential energy provision of the Einstein Equivalence Principle, guaranteed by the locally measured invariance of ϕ, the cornerstone of general relativity. It is also the cornerstone of Mach's principle, though Brans (and his mentor at the time, Robert Dicke) did not understand it that way.

The issue of a more realistic general relativistic calculation of inertial forces can be addressed in two parts. First, the force produced (via frame dragging) by an accelerating sphere of matter with uniform density on its interior contents; and second, by calculation of the "Sciama force" produced by a realistic model of the contents of the universe. The first calculation can be found in a paper by Keneth Nordtvedt on "gravitomagnetism" published in 1988.[3] He found $4GM/R$ for the coefficient of the acceleration. That is, Sciama's calculation, in ignoring the geometric effects of general relativity, is off by a factor of 4. Sultana and Kazanas have recently shown that when realistic cosmological parameters (for example, replacing the Hubble sphere with that particle horizon) are used to calculate the value of ϕ / c^2 in Equation (3), one gets 0.23, rather than one.[4] However, when this result is combined with Nordtvedt's, one finds 0.92 for the coefficient of the acceleration in Equation (4), that is, a value, well within observational error, of one. A value of 0.92, with some modest error, is consistent with the cosmic scale spatial flatness that follows from the Wilkinson Microwave Anisotropy Probe analysis, which implies that $\phi / c^2 = 1$. So, both observation and theory lead to the conclusion that inertial forces and the origin of inertia itself are consequences of the gravitational action of chiefly distant matter in our universe.

II. Mach Effects

When inertial effects are identified as due to the action of the gravitational field with matter sources, it makes sense to ask: what are the local sources of the field when dynamical circumstances (the action of local forces) are present? The simplest way to answer this question is to consider an object being accelerated by an external force, and take the gravitational interaction to be the inertial reaction force it feels divided by the object's mass to get the field strength. In order to keep the force consistent with special relativity, we use the "four" force/mass= $\boldsymbol{F}$=F/m, which includes a time-like part, as well as the customary spatial part, f=$\boldsymbol{E_g}$, of Newtonian dynamics. Dividing the numerator and denominator of the resulting expression by the volume of the object to put the expression in terms of densities, we get:

$$\boldsymbol{F} = -\left(\frac{c}{\rho_0} \frac{\partial \rho_0}{\partial t}, \boldsymbol{f} \right).$$

(5)

The subscript zero indicates the "proper" density, that is, the density as measured in the instantaneous rest frame of the accelerating object. Taking the four-divergence of this field strength gives us the local sources of the field. Using Mach's principle, which requires that $\phi / c^2 = 1$ and concomitantly $\phi = c^2$ so that $\rho \phi = \rho c^2$, the four-divergence of Equation (5) is found to be:

$$\nabla^2\phi - \frac{1}{c^2}\frac{\partial^2\phi}{\partial t^2} = 4\pi G\rho_0 + \frac{\phi}{\rho_0 c^2}\frac{\partial^2\rho_0}{\partial t^2} - \left(\frac{\phi}{\rho_0 c^2}\right)^2\left(\frac{\partial\rho_0}{\partial t}\right)^2 - \frac{1}{c^4}\left(\frac{\partial\phi}{\partial t}\right)^2 \tag{6}$$

This is just the classical wave equation for the scalar potential of the field. Note the transient source terms present in this equation. We can separate them out and write down the expression for the transient mass source as:

$$\delta\rho_0(t) \approx \frac{1}{4\pi G}\left[\frac{1}{\rho_0 c^2}\frac{\partial^2 E_o}{\partial t^2} - \left(\frac{1}{\rho_0 c^2}\right)^2\left(\frac{\partial E_0}{\partial t}\right)^2\right]. \tag{7}$$

The last term on the RHS of Equation (6) has been dropped as it is always minuscule, and the proper matter density in the derivatives has been written as E_0/c^2. If we integrate this over some object to which power P is being applied to find the proper mass fluctuation δm_0, we get:

$$\delta m_0 = \frac{1}{4\pi G}\left[\frac{1}{\rho_0 c^2}\frac{\partial P}{\partial t} - \left(\frac{1}{\rho_0 c^2}\right)^2\frac{P^2}{V}\right]. \tag{8}$$

V in this equation is the volume of the object to which the power is applied. *Note that the mass fluctuation predicted here only occurs in an object that is being accelerated as the power fluctuates. If no "bulk" acceleration of the object takes place, there is no mass fluctuation.* This is a consequence of the fact that the mass fluctuation arises from the divergence of the time-like part of the field strength in Equation (5), the rate at which the field does work on its sources as an acceleration proceeds. That work deposits energy in the bonds that bind the constituent particles, not the particles themselves. So this mass fluctuation does *not* lead to changes in the restmasses of elementary particles.

Acceleration dependence can be restored to Equation (8) explicitly by noting that when a (three) force **F** acts on an object, the change in energy *dE* of the object is given by:

$$dE = \mathbf{F} \bullet d\mathbf{s} \tag{9}$$

So,

$$\frac{dE}{dt} = \mathbf{F} \bullet \mathbf{v} = P \tag{10}$$

And,

$$\frac{dP}{dt} = \mathbf{F} \bullet \mathbf{a} + \mathbf{v} \bullet \dot{\mathbf{F}} \tag{11}$$

where *P* is the power communicated to the object by the applied force and the over-dot indicates differentiation with respect to time. Care must be taken with this analysis, for **v**, which has a simple interpretation in the case of a rigid body acted upon by an external force, is more complicated when the object acted upon can absorb internal energy. We also note that $\dot{\mathbf{F}}$ involves a third time derivative of position and the time derivative of the mass, so, for a lowest order calculation, we set the second term on the RHS of Equation (11) aside. Substituting from Equation (11) into Equation (8), we get:

$$\delta m_0 \approx \frac{1}{4\pi G}\left[\frac{1}{\rho_0 c^2}\frac{\partial P}{\partial t}\right] \approx \frac{1}{4\pi G\rho_0 c^2}\mathbf{F}\bullet\mathbf{a} = \frac{1}{4\pi G\rho_0 c^2}m_0\,a^2 . \qquad (12)$$

Evidently, the simplest Mach effect depends on the square of the acceleration of the body in which it is produced. Note, by the way, that the units of these equations are Gaussian, in keeping with the traditions of field theory of yesteryear. The SI counterpart of this equation does not have the 4π in the denominator on the RHS, though G (in appropriate units) remains the coupling coefficient between sources and fields for gravity.

III. Stationary Forces

If we produce a fluctuating mass in an object, we can, at least in principle, use it to produce a stationary force on the object, thereby producing a propulsive force thereon without having to expel propellant from the object. We simply push on the object whose mass is fluctuating when it is more massive, and pull back when it is less massive. The reaction forces during the two parts of the cycle will not be the same due to the mass fluctuation, so a time-averaged net force will be produced. This may seem to be a violation of momentum conservation. But the Lorentz invariance of the theory guarantees that no conservation law is broken. Local momentum conservation is preserved by the flux of momentum in the gravity field that is exchanged with the chiefly distant matter in the universe. Note that this flux is decades of orders of magnitude larger than that customarily associated with gravity waves. That is because electromagnetic scale forces are those involved in inertial effects, not the utterly minuscule forces associated with conventional gravitational quadrupole radiation, as pointed out above.

IV. Experment

The obvious way to test for the presence of proper matter density fluctuations of the sort predicted in Equations (8) and (12) is to subject capacitors to large, rapid voltage fluctuations. Since capacitors store energy in dielectric core lattice stresses as they are polarized, the condition that E_0 vary in time is met as the ions in the lattice are accelerated by the changing external electric field. If the amplitude of the proper energy density variation and its first and second time derivatives are large enough, a detectable mass fluctuation should ensue. That mass fluctuation, δm_0, is given by Equation (12) above. *Note that the assumption that all of the power delivered to the capacitors ends up as a* proper *energy density fluctuation may be an optimistic assumption.* Nonetheless, it is arguably a reasonable place to start. *Note too that simply charging and discharging capacitors will not produce mass fluctuations. They must at the same time be subjected to large "bulk" accelerations – the acceleration that appears explicitly in Equation (12).*
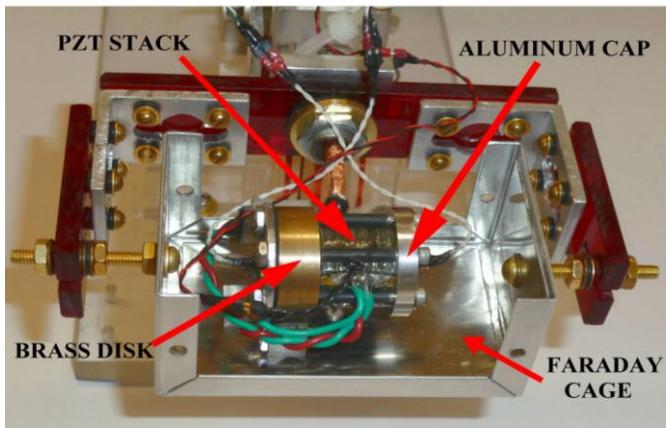

Figure 1. A PZT stack device mounted in a Faraday cage on the beam of a thrust balance.

The way to deal with the latter of these issues, "bulk" accelerations, is to use electromechanical materials to make one's capacitors. That way, while energy is being stored in such a device, a mechanical acceleration of the device is produced by the first order (in the voltage) piezoelectric effect (if present) and the second order electrostrictive effect. In the work reported here, the devices tested consisted of stacks of 19mm diameter by 1 and 2 mm thick lead-zirconium-titanate (PZT) crystals glued together with electrodes. The stacks, with four 2 mm thick crystals at one end and eight 1 mm thick crystals at the other, with embedded accelerometers made with 0.3 mm thick crystals, had a length of 19 mm. Steiner-Martins mixture SM-111 was used to make the crystals. For testing, the PZT stacks were clamped between a thin (4 mm thick) aluminum

end cap and a thicker (9.5 mm thick) brass disk that acted as a reaction mass against which the mechanical action of the stack took place. The end of the stack with the 1 mm thick crystals was placed near the aluminum cap as that was where the greatest accelerations were expected. One of these devices mounted on an aluminum bracket in its Faraday cage on the end of a thrust balance beam is shown in Figure 1. The Faraday cage is an aluminum project box lined with mu-metal, with the top removed in Figure 1 so that the enclosed device can be seen.

The thrust produced by the device shown in Figure (1) was detected using a thrust balance designed to be able to detect thrusts on the order of a few tenths of a micronetwon with only modest signal averaging. The thrust balance was based on a pair of C-flex flexural bearing. It is displayed in Figure 2. Of special note are the galinstan liquid
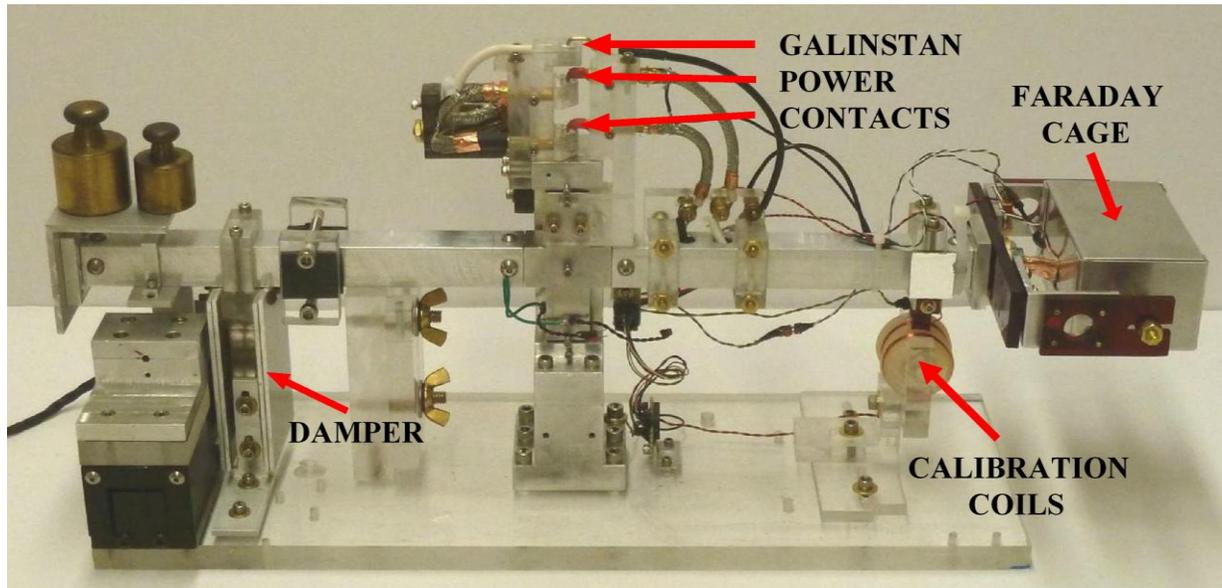
Figure 2. The thrust balance used in the experiment whose results are reported here. C-flex flexural bearings in the central column support the balance beam and provide the restoring torque for thrust measurements. The position of the beam is sensed with a Philtech optical position sensor whose probe is attached to the stepper motor to the left of the damper.

metal contacts located coaxially with the support bearing used to transfer power to the device on the end of the beam. Calibration of the balance is achieved using three 10 turn coils. The two outer coils are affixed to the balance platform; and the third coil is located midway between the outer coils and attached to the balance beam. The coils are wired in series; and a current through them produces a known force on the beam whose displacement by the force is measured with the optical position sensor located at the other end of the beam. The motion of the beam is damped by a pair of aluminum plates attached to the beam that move in the magnetic field of an array of small neodymium-boron magnets. The power circuit was extensively shielded to insure that stray fields did not compromise the results.

The electronics for this experiment fall into three general categories: the power circuit, the instrumentation circuits, and the computer control and data acquisition system. The last of these was based on a Canetics analog to digital converter board (8 A/D channels with 12 bit resolution) supplemented by two digital to analog (D/A) channels. One of the D/A channels was used to switch the power signal to the power amplifier. The other was used to modulate the frequency of the signal generator so that sweeps of selected frequency ranges could be carried out in the data acquisition process. The A/D channels recorded the output of the thrust sensor, the (rectified) amplitude of the voltage across the device, the amplitude of the (rectified) voltage signal generated by the accelerometer embedded in the active part of the PZT stack, and the temperature of the aluminum cap (in immediate proximity to the active part of the PZT stack). Other temperature and accelerometer measurements were made at various times. But for the results reported here, only the aforementioned data channels are relevant.

The power circuit consisted of two parts: the power amplifier, and the signal generator that produced the amplified signal. The signal generator was based on the Elenco Function Blox signal generator board. This board, in addition to allowing the selection of frequency range and signal waveform, provides for both amplitude and

frequency modulation. For this experiment, only the sine waveform was used, and the frequency range was 10 to 100 KHz. Since the effect sought depends on operation at a resonant frequency of the device, frequency modulation was used to scan a range of frequencies so that resonant frequencies could be identified. Since the signal generator is a voltage controlled oscillator, a low voltage signal (a few volts) could be used to control the frequency. And frequency sweeps can be generated by sweeping a small range of low voltages for the control signal. The power amplifier employed was a Carvin DCM 1000 operating in bridged mode.

All of the instrumentation channels were buffered with instrumentation amplifiers (to protect other circuitry and insure that the signal recorded was referenced to local ground) and provided with (50 Hz low pass) anti-aliasing filters. The thrust sensor was also provided with an offset and high gain amplifier (to resolve small signals riding on a ~ 5 volt signal), as these available options had not been purchased with the original Philtech device. Oscilloscopes and meters were employed for real-time monitoring of the AC and DC signals. Oscilloscopes of several varieties were used to real-time monitor various instrumentation channels prior to their rectification by Analog Devices AD-630 synchronous demodulators for storage as simple votage signals. In particular, a 12-bit resolution, 2 channel Picoscope was used to monitor (and capture) the FFT spectra of the device voltage and accelerometer channels. And a GW-Instek digital scope was used to display and capture the corresponding waveforms (at 8-bit accuracy).

V. The Predicted Thrust in PZT Stacks

A stationary thrust was sought in this experiment. As mentioned in section III, the production of such thrusts depends on combining a periodic force on an object undergoing periodic mass fluctuations at the frequency of the fluctuations with an appropriate phase so that the force on the object in one part of each cycle is different from that in another part of the cycle. Initial experiments with PZT stacks of the design mentioned above, carried out in 1999 and 2000, used crystals made by Edo Corporation, made of their mixture EC – 65. This material has both piezoelectric (linear) and electrostrictive (quadratic) voltage responses; but the piezoelectric response is much larger than the electrostrictive response.

According to Equation (12), the mass fluctuation induced by a sinusoidal voltage signal of angular frequency ω will be proportional to the square of the induced acceleration. Since the chief response is piezoelectric (that is, linear in the voltage), the displacement, velocity, and acceleration induced will occur at the frequency of the applied signal. And the square of the acceleration will produce a mass fluctuation that has twice the frequency of the applied voltage signal. In order to transform the mass fluctuation into a stationary force, a second (electro)mechanical force must be supplied at twice the frequency of the force that produces the mass fluctuation. In the work with the Edo based PZT stacks, this second, second harmonic signal was produced by squaring the first harmonic signal and providing offset and phase adjustment capability. While this capability remained a part of the signal conditioning electronics, it was found unnecessary in the work with the Steiner-Martins based PZT stacks, for the electrostrictive response of this material was markedly stronger than that for the EC – 65 material.

Calculation of the interaction of the electrostrictive electromechanical effect with the predicted mass fluctuation is straight-forward. We assume that a periodic current i, given by:

$$i = i_0 \cos \omega t \tag{13}$$

is applied to the PZT stack. We take the power circuit to be approximately a simple series LRC circuit. When such a signal is applied at a frequency far from a resonance of the power circuit, the corresponding voltage will be roughly 90 degrees out of phase with the current. At resonance, where the largest Mach effects can be expected, the relative phase of the current and voltage in the power circuit drops to zero, and:

$$V = V_0 \cos \omega t \tag{14}$$

The length of the PZT stack, x, including the piezoelectric displacement is:

$$x = x_0 \left(1 + K_p V\right), \tag{15}$$

where x_0 is the length for zero voltage and K_p is the piezoelectric constant of the material. The velocity and acceleration are just the first and second time-derivatives (respectively) of Equation (15). The mass fluctuation, accordingly, is:

$$\delta m_0 \approx \frac{1}{4\pi G \rho_0 c^2} m_0 a^2 = \frac{1}{4\pi G \rho_0 c^2} m_0 \left(-\omega^2 K_p x_0 V_0 \cos\omega t\right)^2 = \frac{\omega^4 m_0 K_p^2 x_0^2 V_0^2}{8\pi G \rho_0 c^2}(1+\cos 2\omega t). \quad (16)$$

Keep in mind that in SI units, the factor of 4π must be removed from the denominators in this equation. Electrostriction produces a displacement proportional to the square of the applied voltage, or:

$$x = x_0\left(1 + K_e V^2\right) = x_0\left(1 + K_e V_o^2 \cos^2 \omega t\right), \quad (17)$$

where K_e is the electrostrictive proportionality constant. Using the customary trigonometric identity and differentiating twice with respect to time to get the acceleration produced by electrostriction,

$$\ddot{x} = -2\omega^2 K_e x_0 V_0^2 \cos 2\omega t \quad (18)$$

The force on the reaction mass (the brass disk in this case) is just the product of Equations (16) and (18):

$$F = \delta m_0 \ddot{x} \approx \frac{\omega^6 m_0 K_p^2 K_e x_0^3 V_0^4}{4\pi G \rho_0 c^2}(\cos 2\omega t)(1+\cos 2\omega t). \quad (19)$$

Carrying out multiplication of the trigonometric factors and simplifying:

$$F = \delta m_0 \ddot{x} \approx \frac{\omega^6 m_0 K_p^2 K_e x_0^3 V_0^4}{8\pi G \rho_0 c^2}(1+2\cos 2\omega t + \cos 4\omega t). \quad (20)$$

The trigonometric terms time-average to zero. But the the first term on the RHS of Equation (20) does not. The time-average of F is:

$$\langle F \rangle \approx \frac{\omega^6 m_0 K_p^2 K_e x_0^3 V_0^4}{8\pi G \rho_0 c^2} \; . \quad (21)$$

Remember that Equations (20) and (21) are only valid at resonance when the current and voltage in the circuit are in phase; and that a factor of 4π must be removed from the denominator if SI units are used. This is the thrust signal sought in this experiment.

To get a sense for the type of thrusts predicted by the larger Mach effect, we substitute values for a PZT stack device used in the experimental work reported here into Equation (21). The resonant frequencies for this type of device falls in the range of 35 to 40 KHz, and we take 38 KHz as a nominal resonant frequency. Expressing this as an angular frequency and raising it to the sixth power, we get 1.9 X 10^{32}, a rather large number. The mass of the PZT stack is 46 gm. But only a part of the stack is active, say, 25 gm, or 0.025 kg. The length of the stack is 19 mm; but a typical value for the active part of the stack is roughly 15 mm, or 0.015 m. In most circumstances the voltage at resonance is about 200 volts. And the density of SM-111 material is 7.9 gm/cm^3, or 7.9 X 10^3 kg/m^3. We use the SI values of G and c, and set aside the values of the piezoelectric and electrostrictive constants for the moment. Inserting all of these values and executing the arithmetic:

$$\langle F \rangle \approx 3.4\times 10^{23} K_p^2 K_e. \quad (22)$$

Steiner-Martins gives 320 X 10^{-12} m/Vfor the "d_{33}" piezoelectric constant of the SM-111 material. That is, K_p has this value. Note, however, that the dimensions given are not correct. The piezoelectric constant does not have the dimension of meters because the spatial dependence is "fractional". That is, the constant contains spatial dependence as change in meters per meter, which is dimensionless.

Steiner-Martins lists no value for the electrostrictive constant. But electrostrictive effects are generally smaller than piezoelectric effects. When the stated value for K_p is inserted into Equation (22) we get:

$$\langle F \rangle \approx 3.5 \times 10^4 \, K_e. \tag{23}$$

If we take the electrostrictive constant to be roughly the same as the piezoelectric constant, we find that a thrust of about 11 micronewtons is predicted. As shown below, the observed thrust for these circumstances is a few micronewtons. That is, prediction and observation agree to order of magnitude. Two issues, however, should be kept in mind. One is that the electrostrictive constant is likely smaller than the piezoelectric constant. The other is that mechanical resonance amplification doubtless takes place at the mechanical resonance frequency. Resonance was taken into account in the relative phase of the current and voltage in the power circuit. But no allowance for mechanical resonance amplification was made. Since the mass fluctuation goes as the square of the acceleration, even modest resonance apmplification can have noticeable effects. These considerations are competing effects, and as such, taken together, are unlikely to radically change the prediction we have computed here.

We remark that the result of this calculation is very different from that of other calculations for similar circumstances. In those calculations δm_0 was calculated using Equation (8) and the electrical properties of the system being considered without regard to the details of the accelerations present in the system. The mechanical behavior of the system is then supplied separately in the second harmonic force rectification process. Doing things this way, for example, leads to the prediction of thrust of a tenth of a Newton or more for systems like the PZT stacks addressed here. In light of the calculation based on explicit acceleration dependence, it would appear that this other method of calculating Mach effects is fundamentally flawed and should be avoided.

VI. Experimental Protocols

When experiments with PZT stacks were first designed over a dozen years ago, two procedures were used in collecting data. Sweeps of chosen ranges of frequencies were done, chiefly to identify the presence and locations of resonant behaviors. Once found, the frequency of the applied signal(s) was adjusted to the resonant frequencies (one at a time) and sustained pulses of power with a half second to several seconds duration were administered. In addition to the applied voltage and thrust response, several other data channels were recorded – including the response of an accelerometer embedded in the PZT stack and the temperature measured with a thermistor embedded in the aluminum cap that clamps the stack to the brass reaction disk. The cycles of data were computer controlled so as to be identical to each other, simplifying the task of signal averaging with multiple cycles to suppress random noise in the data.

Data were acquired at a rate of 100 Hz per channel, and each channel was provided with a 50 Hz low pass anti-aliasing filter. In the present work, started a year and a half ago, data cycles of 20 seconds were initially used, and recently the interval was extended to 32 seconds. Instead of doing frequency sweeps and pulses separately, they were combined. Each cycle consisted of a few seconds of quiescent initial data, followed by a power pulse at the center frequency of the sweep to follow with a duration of a half second to several seconds, followed by the frequency sweep of a predetermined range, followed by another center frequency pulse like the initial one, followed by several seconds of quiescent data. Usually, but not always, the center frequencies for the sweeps were chosen to be resonant frequencies of the devices. Typically, between one and two dozen cycles of data taken under the same circumstances (durations and center frequencies, but not things like temperature) were needed for signal averaging that would reduce the noise in the thrust traces to a few tenths of a micronewton or less. After the resonance frequency of a particular PZT stack was established, runs were sometimes done without frequency sweeps. In one case, in the normally swept part of each cycle the device was simply turned off. In another case, the normally swept part of the cycle was replaced with constant center frequence power on, resulting in a power pulse of 10 seconds duration. Since the settling time of the balance beam was about 5 seconds, these 10 second power pulses allowed the demonstration of the stationary nature of the thrusts produced by the Mach effect in these devices.

The resonant frequencies for the PZT stacks were found to lie in the range of 35 to 40 KHz. Though it was not appreciated at the outset, the electrical and mechanical resonant frequencies in this range did not necessarily coincide, depending on detailed circumstances differing by as much as a kilohertz or two. When, by chance, they did coincide, unusually good behavior was obtained. One device, in which the two resonances coincided by chance for a while, produced thrusts on the order of 10 μN for several weeks, the amplitude of the voltage across the device at resonance being in the range of 350 to 400 volts. The "just so" conditions were eventually lost. But this and another device like it continued to produce thrusts up to a couple of μN, and those devices were used to carry out a series of tests to establish whether the thrust signals spurious, or evidence for a real Mach effect.

Those tests included checking to see whether the thrusts seen depended on the pressure of the residual air in the vacuum chamber by comparing data obtained with the chamber pressure less than 10 mT with data for a chamber pressure of 10 T. No significant difference was found. Mechanical thrust signals were generated using the calibration system so that mechanical signals, which are affected by the inertia of the balance beam, could be consistently discriminated from, for example, electrical signals. Another test involved replacing the device with a capacitor with roughly the same capacitance (41 nf versus 39 nf) as the devices and running to see what effect the currents and voltages present had on the thrust circuit. The simple answer is, none. Another test involved removing part of the Faraday cage and carrying out thrust tests with the device in various orientations to see if there was any electromagnetic coupling to insulators or conductors in the environment. None was detected.

One routine test and two potential spurious sources of signals deserve special mention. The routine test was reversal of the direction of the device on the balance beam; that is, "forward" and "reversed". Essentially all data was acquired with roughly equal numbers of cycles of forward and reversed orientations. The reason for following this protocol is simple. When the difference of the forward and reversed averages is taken, all signals that do not reverse sign with the direction reversal are cancelled as common mode "noise". For example, should a small torque be introduced by the currents and/or voltages present in the galinstan contacts or their leads, they will not change when the direction of the device is reversed. Consequently, they will be cancelled by this protocol. Likewise for all other non-reversing signals. And one can have confidence that any thrust that survives this protocol is produced in the device and/or its mount and Faraday cage, for they are the only things that change with direction reversal.

The two sources of potential spurious signals are thermal effects and "Dean drive" effects. Operation of the devices causes them to heat up. That in turn causes thermal expansion of the parts of the device and its mount. And the thermally driven motion of the parts of the device and mount, if they are changing in time, will produce thrusts that are communicated to the balance beam. In the case of Dean drive effects, vibration – and inevitable accompaniment to the operation of the devices – if it is communicated to a part of the balance where static and dynamic friction can act periodically to cause motion in one direction (but not the other), can produce behavior that looks like a thrust acting on the balance beam. This may take place, for example, with an object experiencing eccentric motion sitting on a rough surface, or located in a fluid with non-vanishing viscosity. In the case of this apparatus, the test that excludes residual air in the vacuum chamber eliminates the fluid variety of Dean drive effect. The only other place where such an effect might operate is in the bearings that support the balance beam in the central column. A careful investigation of both of these effects was carried out by one of us (JFW), and the results are reported in detail in the forthcoming book: *Making Starships and Stargates: the Science of Traversable Absurdly Benign Wormholes*.[5] Here we report subsequent work that encompasses data that speaks to the issue of thermal effects in a different way than than previously reported.

VII. Results

After the experimental results reported in Ref. 5 were obtained, several system failures occurred. Upgrades to the data acquisition system in particular were required. The down-time mandated by these activities gave the test devices time to undergo relaxation. When, after several weeks, everything was restored, we found that the behavior of one of the main devices had measurably improved. And upgrades other than those to the data acquisition system had improved the noise level in the system enough to make averages of 10 to 12 cycles of data sufficient to suppress noise to negligible levels.

A. Short Power Pulses and Frequency Sweeps

The first sequence of runs was done using the forward/reversed protocol for one second pulses at the beginning and end of the 8 second interval during which frequency sweeps were performed. The averages of this data for the forward and reversed device directions are dislayed in Figure 3. In this figure the red traces are thrust, the blue are the square of the voltage across the device (proportional to power), and the lavender traces track the temperature of
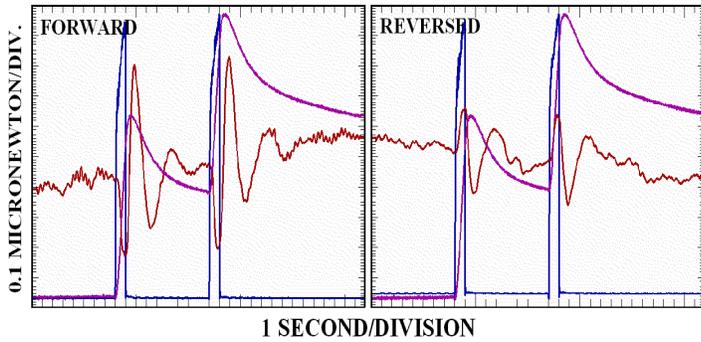
Figure 3. The thrust traces (red) for the forward and reversed orientations of the device on the balance beam. Blue is power and lavender, temperature.

the aluminum cap clamped to the active end of the PZT stack. The voltage/power traces rise during the powered one second intervals because these cycles were done with the device "cold" (near room temperature) as at that temperature the best results were obtained. This is a consequence of the fact that the thermal expansion of PZT in the direction of polarization is negative; that is, contraction with increasing temperature. This behavior degrades the preload condition and, concomitantly, the mechanical behavior. The temperature traces are exactly what one would expect: steady heating while in operation, followed by exponential cooling. The total temperature rise is a few degrees Celsius.

The underlying thrust pulse in these data has an amplitude of about 2.5 micronewtons – easily seen, even in a single cycle, but small enough so that any asymmetry in the response of the balance beam competes with the signal. Here, this is manifested by the forward and reversed thrust pulses being of unequal amplitude. The likely cause of this asymmetry is the bundle of instrumentation leads that run from the beam to the balance platform near the central column of the balance, shown in Figure 4. This effect amounts to the presence of a non-reversing thrust, and it is eliminated when the forward and reversed thrust data are differenced as described above. That process yields the net thrust trace presented in Figure 5. Evidently, a thrust pulse is produced in this device when it is driven with a 38 Khz signal of sufficient amplitude. But without prior knowledge of the tests already done to exclude mundane effects, it is easy to believe that the thrusts seen might be due to some cause other than the Mach effect – in particular, it might be due to a thermal effect, for the effects produced by thermal expansion of the PZT stack reverse direction with the device.

Thermal effects have been thoroughly excluded through analysis of their dynamical effects (see Ref. 5). By
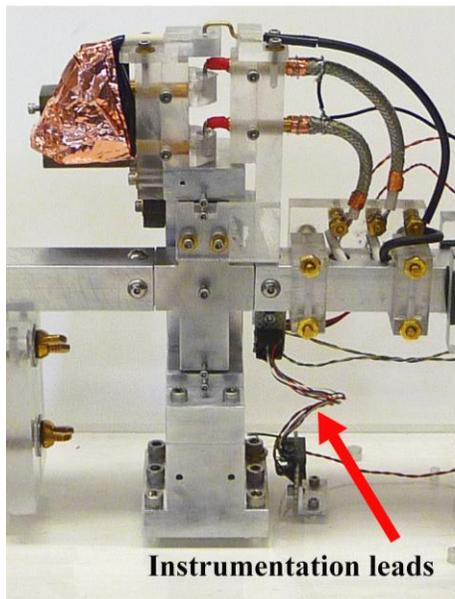

Figure 4. Detailed view of the central column. The instrumentation leads are to the right of the column; and the galinstan contacts above it.
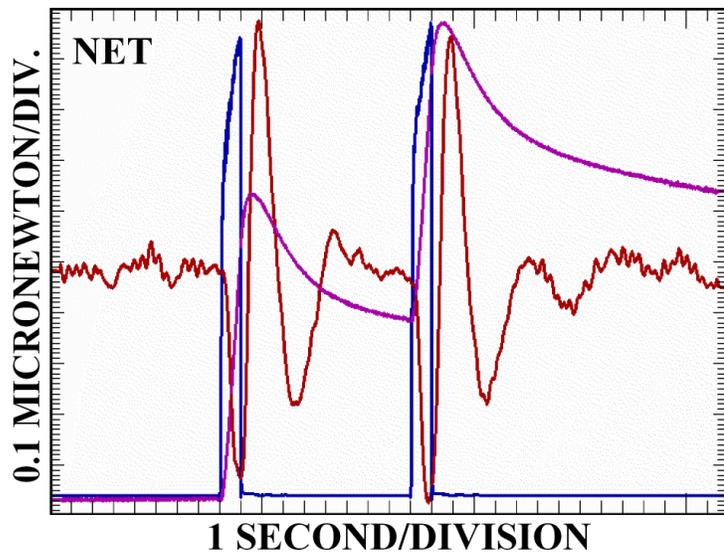
Figure 5. The net trust trace (red) – the difference of the forward and reversed thrust traces shown in Figure 3 – produced by this device with a voltage amplitude of 200 volts at 38 KHz. Note that the settling time is about 5 seconds.
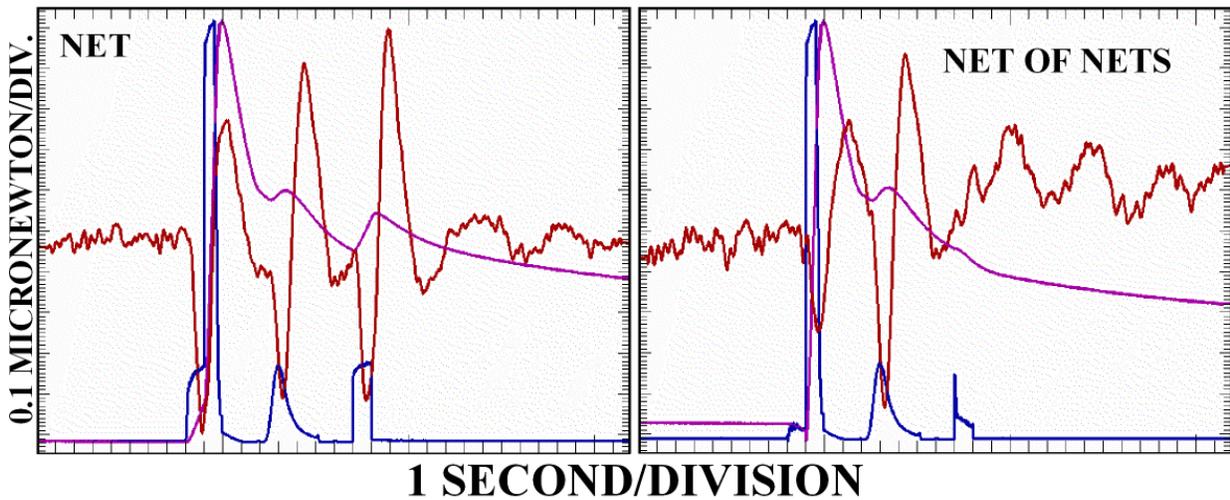
chance, however, when frequency sweeps were done with the present device, its relaxation for several weeks brought out an unexpected behavior that makes the exclusion of thermal effects almost trivial. The behavior in question was first encountered with the first of the Steiner-Martins devices more than six months ago. It depends on the fact that the electrical and

11

American Institute of Aeronautics and Astronautics
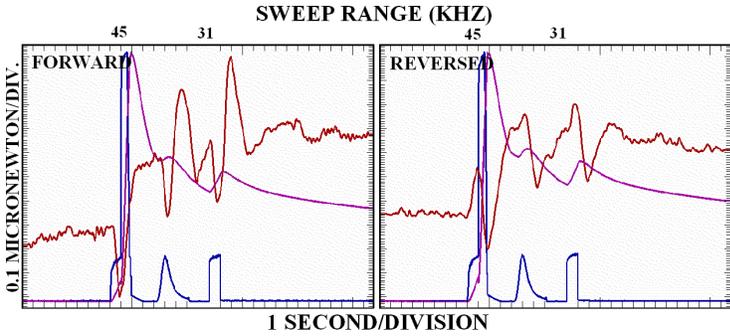
Figure 6. Averages of forward and reversed orientation cycles for runs done with a 14 KHz frequency sweep centered on 38 KHz between the constant frequency power pulses. Thrust traces are red and power, blue.

mechanical resonances in these devices do not necessarily occur at exactly the same frequencies. When, by chance, they do happen to coincide, spectacular behavior results. In effect, coincidence tunes the power circuit, and much larger voltages across the devices are produced with smaller gains of the power amplifier. In earlier work, this behavior could only be reliably produced when the electrical/mechanical coincidence happened to be at the chief mechanical resonance. For this device, that frequency is 38 KHz. But when frequency sweeps were done with the present system, the results for forward and reversed averages are those displayed in Figure 6. As you can see, at the onset of the sweep "just so" conditions produce a power spike (blue trace) roughly more than five times as large as the power response at the center, mechanical resonance


Figure 7. The net thrust trace, forward minus reversed, for the cycle averages done with frequency sweeps between the center frequency pulses is shown in the left panel. Note that the very large power and temperature pulses are not accompanied by a corresponding thrust pulse. In the right panel, the difference between the thrust trace in the left panel and that in Figure 5 is shown. The thrust pulses produced by the beginning and ending center frequency pulses are completely cancelled, whereas the thrust pulse at the center of the sweep is not. Only a small thrust pulse accompanies the anomalous power and temperature spike at the beginning of the sweep, whereas were the thrust pulses cause by thermal effects, a thrust pulse an order of magnitude larger would be expected.

frequency. This power spike – that generates a thermal pulse (lavender trace) far larger than those produced by the on resonance power pulses – however, produces almost no thrust pulse of the sort that the on resonance power pulses produce. What it does do for both the forward and reversed thrusts is cause a secular upward shift of the thrust traces, a non-reversing with direction effect that is cancelled when the thrust traces are differenced. This is shown in the left panel of Figure 7. Thrust pulses like those in Figure 5 accompany the beginning and ending center frequency power pulses. And a similar thrust pulse is produced as the center frequency is swept 13 seconds into each cycle. There is a trace of some upward drift of the thrust trace during the powered interval. But there is no large secular upward shift as is present in the forward and reversed results in Figure 6. More importantly, whereas large thrust pulses accompany the small bumps in the lavender temperature trace in Figures 6 and 7 left, none is present for the very much larger temperature spike that accompanies the power spike at the beginning of the sweep.

The easiest way to show the absence of a thrust pulse proportional to the power and temperature spikes at the beginning of the frequency sweep is to subtract the net thrust without the sweep from the net thrust with the sweep. This is shown in the right panel of Figure 7. The expected thrust pulse, were the thrust pulses due to a thermal effect, already absent in Figures 6 and 7 left, is conspicuously not present in Figure 7 right. It follows that the thrusts that accompany on resonance operation of the PZT stack cannot be attributed to thermal effects.

B. Long Power Pulses

Another way of showing of that the thrusts produced in PZT stacks operating in appropriate conditions are not thermal is to show that the thrusts produced are stationary. That is, when the device is turned on, the thrust is steadily produced as long as power is supplied. In the case of thermal effects, the heating rate must be changing for a thrust to be produced. Steady heating produces a steady thermal expansion. But this is a velocity, not the acceleration required to produce a force. Accelerations are also required to produce Mach effects and thrusts
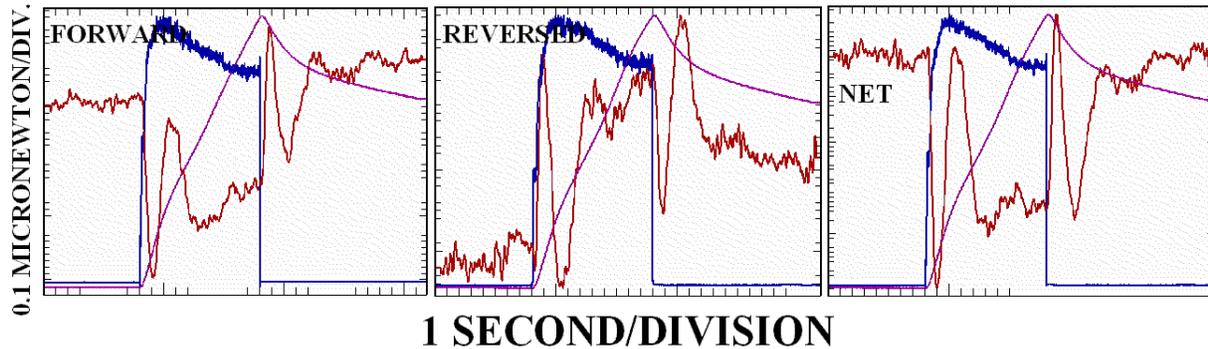
Figure 8. The results for 10 second power pulses on the 38 KHz resonance frequency. Forward orientation is shown in the left pan el, and reversed orientation in the center panel. The upward drift of the thrust traces suggests the presence of secular heating like that in Figure 6. The net thrust trace in the right panel nonetheless shows the predicted stationary thrust during the powered interval. This behavior is incompatible with an effect of thermal origin.

therefrom. But the accelerations can be periodic while producing a thrust in one direction. To test this prediction, we have collected data where power was delivered to the PZT stack for a 10 second interval. Since the settling time of the balance is about 5 seconds, the 10 second interval is sufficient to demonstrate the predicted behavior. The various averages computed with this data are presented in Figure 8. Suffice it to say that the predicted stationary thrust behavior is present.

C. The Predicted Thrust

One issue remains to be dealt with: the predicted thrust. In section V we found that:

$$\langle F \rangle \approx 3.5 \times 10^4 \, K_e. \tag{23}$$

When the piezoelectric constant for SM-111 was used for K_e, a thrust of 11 micronewtons was obtained. Observation gives a thrust of 2 to 3 micronewtons. So, since no reported value for K_e is available, the question is: can we estimate the value of K_e from some measurement? If K_e is within an order of magnitude or two of K_p, we can do this by measuring the relative magnitudes of the first and second harmonics of the motion of the PZT stack. The fact of the matter is that should you watch in real time the waveforms of the voltage sense and stack accelerometer circuits, or the spectra of those waveforms you would find that there is "typical" behavior accompanied by some noticeable fluctuation. The fluctuations are sufficiently quick and short-lived that the nature of the fluctuations cannot be ascertained in real-time observation. But they can be isolated recording and playing back in slow motion the recorded behavior. How these fluctuations figure in to the production of thrust in these devices is not known and is a matter for further investigation. Since the dominant behavior is "typical", we shall assume that it is responsible for the thrusts reported here. That behavior is displayed in Figure 9. The left panel of

this figure shows typical waveforms for the device voltage (blue) and stack accelerometer (yellow). The voltage trace is only slightly distorted from a pure sine wave. But the accelerometer trace is clearly not a simple, single frequency sinusoid. These observations are confirmed by examination of the spectrum that corresponds to the wave-forms. The voltage spectrum (blue) shows a well-defined signal at 38 KHz and a more smeared response at the second harmonic down 20 dBu (that is, an order of magnitude) from the first harmonic. The accelerometer response (red) mimicks the harmonic voltage response, save for the fact that the second harmonic is only down 13 dBu from
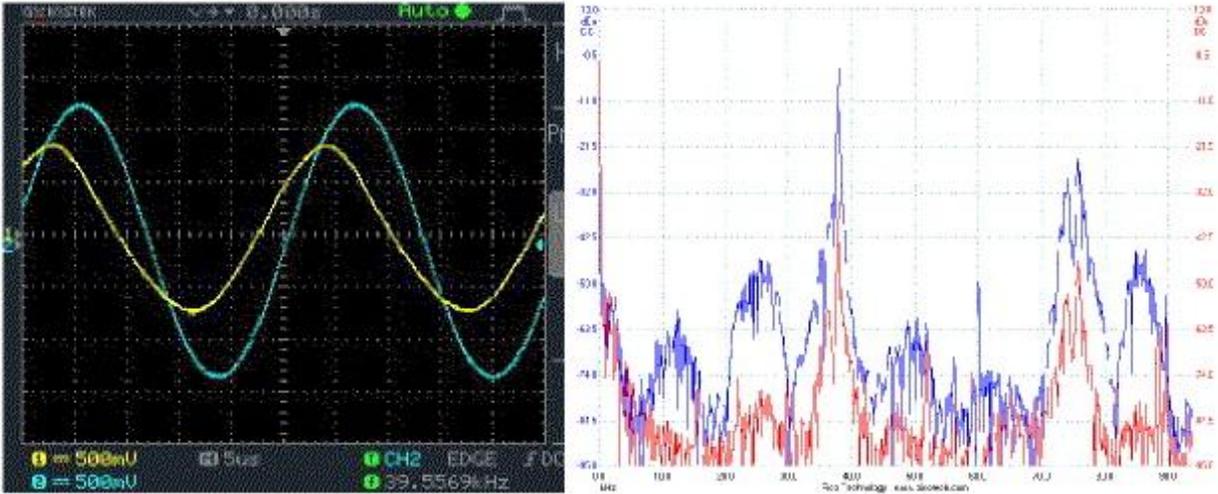
Figure 9. Typical waveforms for the stack voltage (blue) and accelerometer (yellow) are displayed on the left. A corresponding spectrum is displayed on the right. The blue trace is the stack voltage spectrum, and the red trace that for the accelerometer.

the first harmonic – that is, a factor of 0.29 rather than a factor of 0.10. The difference is easily understood. The driving signal is a single frequency sine wave. It drives the piezoelectric response at the first harmonic, but no response at the second harmonic. It also drives the mechanical electrostrictive response at the second harmonic. And that mechanical action produces a piezoelectric voltage that is recorded as the second harmonic voltage response. The important point here, though, is that when the piezoelectric constant is reduced by a factor of 0.29 to correctly replicate the electrostrictive constant, the thrust prediction goes from 11 to 3.2 micronewtons, a value very nearly that observed. Not only does the thrust behavior display the qualitative features expected of a Mach effect thrust, it also is present at the predicted level.

VIII.   Conclusion

We have seen that when the results of the Wilkinson Microwave Anisotropy Probe project are taken into consideration, together with the work of Dennis Sciama, Carl Brans, Keneth Nordtvedt, and others, it follows that inertial forces are gravitational in origin. Moreover, an inertial effect that results from the acceleration of bodies with changing internal energies produces fluctuations in the restmasses of the accelerating objects. Those fluctuating restmasses can be used to demonstrate the reality of these "Mach" effects, as described above. That demonstration involves only one of the two Mach effects predicted by theory. But if it is present, then the other effect must exist too. And if it exists, then in principle it should be possible to produce the gargantuan amount of exotic matter needed to make starships and stargates technically feasible. We therefore recommend that the exploration of Mach effects be pursued with resolve.

Acknowledgments

We thank Keith Wanser for helpful conversations and Thomas Mahood for the construction of the first version of the torsion balance used in the experimental work reported here. Nembo Buldrini and Paul March have also provided help on several technical matters.

References

[1] Sciama, D.W., "On the Origin of Inertia," *Monthly Notices of the Royal Astronomical Society*, Vol. 113, 1953, pp. 34 – 42.

[2] Brans, C.H., "Mach's Principle and the Locally Mesured Gravitational Constant in General Relativity," *Physical Review*, Vol. 125, 1962, pp. 388 – 396.

[3] Nordtvedt, K., "Existence of the Gravitomagnetic Interaction," *International Journal of Theoretical Physics*, Vol. 27, 1988, pp. 1395 – 1404.

[4] Sultana, J. and Kazanas, D., "The Problem of Inertia in Friedmann Universes," 2011, arXiv:1104.1306v.

[5] Woodward, J.F., *Making Starships and Stargates: the Science of Traversable Absurdly Benign Wormholes*, Springer-Verlag, New York, in the press.